

Generation of high-energy-resolved NH_3 molecular beam by a Stark decelerator with 179 stages

Bin Wei(魏斌), Shunyong Hou(侯顺永), Hengjiao Guo(郭恒娇), Yabing Ji(纪亚兵), Shengqiang Li(李胜强), Jianping Yin(印建平)

Citation: Chin. Phys. B . 2019, 28(5): 053701. **doi:** 10.1088/1674-1056/28/5/053701
Journal homepage: http://cpb.iphy.ac.cn; http://iopscience.iop.org/cpb

What follows is a list of articles you may be interested in

Laser-assisted Stark deceleration of CaF in its rovibronic ground (high-field-seeking) state

Yuefeng Gu(顾跃凤), Kai Chen(陈凯), Yunxia Huang(黄云霞), Xiaohua Yang(杨晓华)
Chin. Phys. B . 2019, 28(4): 043702. **doi:** 10.1088/1674-1056/28/4/043702

Optical Stark deceleration of neutral molecules from supersonic expansion with a rotating laser beam

Yongcheng Yang(杨永成), Shunyong Hou(侯顺永), Lianzhong Deng(邓联忠)
Chin. Phys. B . 2018, 27(5): 053701. **doi:** 10.1088/1674-1056/27/5/053701

Tuning the velocity and flux of a low-velocity intense source of cold atomic beam

Shu Chen(陈姝), Ying-Ying Li(李营营), Xue-Shu Yan(颜学术), Hong-Bo Xue(薛洪波), Yan-Ying Feng(冯焱颖)
Chin. Phys. B . 2017, 26(11): 113703. **doi:** 10.1088/1674-1056/26/11/113703

Production of cold CN molecules by photodissociating ICN precursors in brute-force field

Wen-Xia Xu(徐文霞), Yong-Cheng Yang(杨永成), Lian-Zhong Deng(邓联忠)
Chin. Phys. B . 2017, 26(5): 053702. **doi:** 10.1088/1674-1056/26/5/053702

Microwave-mediated magneto-optical trap for polar molecules

Dizhou Xie(谢笛舟), Wenhao Bu(卜文浩), Bo Yan(颜波)
Chin. Phys. B . 2016, 25(5): 053701. **doi:** 10.1088/1674-1056/25/5/053701

Generation of high-energy-resolved NH_3 molecular beam by a Stark decelerator with 179 stages*

Bin Wei(魏斌)[1], Shunyong Hou(侯顺永)[1], Hengjiao Guo(郭恒娇)[1], Yabing Ji(纪亚兵)[1], Shengqiang Li(李胜强)[2], and Jianping Yin(印建平)[1,†]

[1] *State Key Laboratory of Precision Spectroscopy, East China Normal University, Shanghai* 200062, *China*
[2] *School of New Energy and Electronic Engineering, Yancheng Teachers University, Yancheng* 224051, *China*

(Received 5 January 2019; revised manuscript received 8 March 2019; published online 4 April 2019)

We demonstrate the production of cold, slow NH_3 molecules from a supersonic NH_3 molecular beam using our electrostatic Stark decelerator consisting of 179 slowing stages. By using this long Stark decelerator, a supersonic NH_3 molecular beam can be easily decelerated to trappable velocities. Here we present two modes for operating the Stark decelerator to slow the supersonic NH_3 molecules. The first is the normal mode, where all 179 stages are used to decelerate molecules, and it allows decelerating the NH_3 molecular beam from 333 m/s to 18 m/s, with a final temperature of 29.2 mK. The second is the deceleration-bunch mode, which allows us to decelerate the supersonic NH_3 beam from 333 m/s to 24 m/s, with a final temperature of 2.9 mK. It is clear that the second mode promises to produce colder (high-energy-resolution) molecular samples than the normal mode. Three-dimensional Monte Carlo simulations are also performed for the experiments and they show a good agreement with the observed results. The deceleration-bunch operation mode presented here can find applications in the fields of cold collisions, high-resolution spectroscopy, and precision measurements.

Keywords: Stark deceleration, molecular beams, cold molecules

PACS: 37.20.+j, 37.10.Mn, 32.60.+i **DOI:** 10.1088/1674-1056/28/5/053701

1. Introduction

Inspired by the spectacular achievements in cold atoms, the field of cold molecules has been developed rapidly during the last two decades. It has had a significant impact on modern atomic, molecular, and optical physics, physical chemistry, and fundamental physics,[1,2] and offers new applications and potentials in many fields, such as cold collisions[3–5] and cold chemistry,[6–9] high-resolution spectroscopy,[10,11] precision measurements,[12–14] and so on.

A variety of techniques to produce cold molecules have been developed, including buffer-gas cooling,[15] electrostatic Stark deceleration,[16] Zeeman deceleration,[17,18] optical Stark deceleration,[19] Rydberg–Stark deceleration,[20,21] laser cooling,[22–26] and optoelectrical cooling.[27] The Stark deceleration originates from linear accelerators for charged particles, and achieves full control over the velocity and velocity spread of a polar molecular beam. The first experimental demonstration of Stark deceleration was implemented in 1999, in which a pulse beam of metastable CO molecules was decelerated from 225 m/s to 98 m/s.[16] Since then, a number of molecular species have been decelerated,[28–39] trapped,[20,28,40,41] and employed to important applications.[3,10,11,42] Furthermore, different kinds of decelerators have been designed and constructed, including alternating-gradient (AG) decelerator,[43] chip decelerator,[44] traveling wave decelerator,[45,46] ring Stark decelerator,[47,48] and U-shaped decelerator.[49]

The NH_3 molecule is a very promising candidate in molecular physics and physical chemistry and has a variety of applications in the fields of microwave frequency standard, precision measurements, and cold collisions. First, NH_3 was employed in the first atomic clock by Condon and Lyons in 1948[50] and the first demonstration of the microwave amplification by stimulated emission of radiation (maser) by Gordon *et al.* and other groups in 1954–1956,[51–54] and its hyperfine structure in a two-cavity maser was studied in some detail.[55] However, because the central velocities of NH_3 molecular beams were fast and their temperatures were high in these experiments, the performance of the NH_3 maser was considerably limited. It is clear that if the NH_3 molecular beam can be slowed to a very low velocity and cooled to a lower temperature, then the performance of the NH_3 maser will be greatly improved. Next, NH_3 molecule can be used to realize precision measurements[42] in the molecular beam or fountain experiments, such as testing proton–electron mass ratio (m_p/m_e) and its time-variation,[56] time-reversal symmetry, and study the tunneling inversion, as well as near degeneracies between inversion and rotation energy,[57] and so on. Moreover, the high-energy-resolved cold NH_3 molecular beam can also be used to study cold collisions and cold chemistry; for example,

*Project supported by the National Natural Science Foundation of China (Grant Nos. 91536218, 11034002, 11274114, 11504112, and 11504318), the National Basic Research Program of China (Grant No. 2011CB921602), the Fundamental Research Funds for the Central Universities, China, Shanghai Pujiang Talents Plan, China (Grant No. 18PJ1403100), and Exploration Funds for the Shanghai Natural Science Foundation, China (Grant No. 18ZR1412700).

†Corresponding author. E-mail: jpyin@phy.ecnu.edu.cn

© 2019 Chinese Physical Society and IOP Publishing Ltd

measuring the collision cross section and studying its dependence on collision energy.[58,59]

In 2002, the Meijer group first used a traditional Stark decelerator to generate a cold NH_3 molecular beam.[29] However, due to the relatively large inversion splitting, it is more difficult to decelerate the NH_3 molecule than ND_3. To solve this problem, Bethlem group used a complex setup, consisting of a 100-stage traditional Stark decelerator, together with a 336-ring traveling wave decelerator, to slow the NH_3 molecular beam and trap the molecules in the traveling wave decelerator in 2013.[41,60] More recently, they were the first to demonstrate a molecular fountain with NH_3 molecules by using the previously mentioned two types of Stark decelerators, and a combination of quadrupole lens and bunching elements, and they obtained very cold NH_3 molecules.[42] It is well-known that the traveling wave decelerator has many advantages but it is more challenging to implement than the traditional Stark decelerator due to its complex and expensive high-voltage analog amplifiers and electronic controlling system, thus it is difficult to realize traveling wave deceleration for molecules in many laboratories. Consequently, it would be interesting and worthwhile to find a simple experimental setup to realize an efficient deceleration for a supersonic NH_3 molecular beam.

In this paper, we implemented the deceleration of NH_3 molecules with our 179-stage traditional Stark decelerator to obtain a sufficient cold, slow NH_3 packet that can be captured in traps for the applications in cold collisions or high-resolution spectroscopy. The initial supersonic beam of NH_3 was slowed down when the decelerator was operated in the normal mode and the deceleration-bunch mode, respectively. Three-dimensional (3D) Monte Carlo (MC) simulations were also performed for the experiments. Several improvements were presented to increase the number of the desired slow molecules for further applications.

2. Experimental setup

Our schematic experimental diagram is shown in Fig. 1. A supersonic molecular beam of NH_3 molecules is generated by expanding a gas mixture of xenon containing 4.7% NH_3 into vacuum through a 0.5 mm diameter nozzle of a pulse valve (General valve series 90) from a stagnation pressure of 1.5 bar and a temperature of 293 K. The valve operates with a duration of 260 μs leading to a pressure typically up to 1.5×10^{-4} Pa in the source chamber. The initial molecular beam is centered at a velocity of 338 m/s with a full width at half maximum (FWHM) spread of 19%. The beam passes through a 2-mm-diameter skimmer located 22.5 mm downstream from the pulse valve into the second chamber, and then enters a 40-mm-long hexapole which consists of six 3-mm-diameter stainless steel rods evenly placed around a circle with an inner radius of 3 mm. The head of the hexapole is placed 53.5 mm downstream from the pulse valve. After exiting the hexapole, the molecules enter the Stark decelerator with 180 stages. Each stage is formed by a pair of 3-mm-diameter polished parallel cylindrical steel rods, spaced 2 mm apart. The neighboring stages are separated by a center-to-center distance of 6 mm. From the section view of the decelerator, the orientation of the odd-numbered parallel stages and that of the even-numbered parallel ones intersect at 90°, to some extent, making the molecules confined in both transverse directions. All the stages form an array approximately 108 cm long in the beam direction. In each stage, the two rods are connected to two high-voltage power supplies with opposite polarity via the fast high-voltage switches (Behlke Elektronik HTS 201–03-GSM HFB), respectively. The same polarity rods in all the odd-numbered stages are electronically connected, so do the even-numbered stages. Therefore, a total of four independent high-voltage switches and two high-voltage power supplies are required in our deceleration experiments.

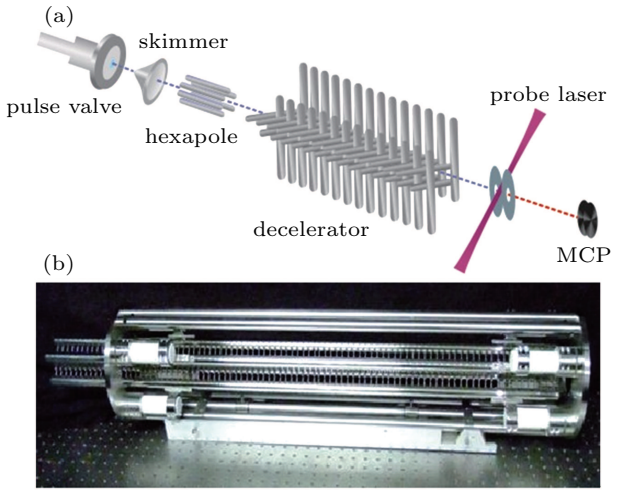


Fig. 1. (a) Schematic diagram of the experimental setup. (b) Our home-made electrostatic Stark decelerator with 179 deceleration stages.

After exiting the decelerator, the molecules are state-selectively detected in the area about 46 mm downstream from the last stage of the decelerator by using the (2+1) resonance–enhanced multi-photon ionization (REMPI) scheme with a focused dye laser (PrecisionScan of Sirah Laser und Plasmatechnik GmbH, pumped by pulse Nd: YAG laser of Quanta-Ray PRO-Series) near 322 nm.[42]

3. Deceleration experiments

The working principle of the Stark decelerator has been discussed in detail elsewhere.[29,61,62] In our experiments presented here, the Stark decelerator is used with different modes of operation, including the guiding mode, the bunching mode, the normal deceleration mode, and the deceleration-bunch mode. The deceleration-bunch mode can be used to improve the energy-resolution of the resulting beam and was firstly demonstrated by Parazzoli *et al.*[63]

3.1. The population and Stark shifts of NH_3 molecule

Because of the adiabatic expansion in the process of producing the supersonic beam, most of NH_3 molecules in the beam reside in the lowest rotational levels in the vibrational and electronic ground state. To acquire a quantitative understanding of the populations in different levels, we calculate the thermal distribution of the rotational levels of NH_3 for different rotational temperatures according to the function[64]

$$N_J \propto (2J+1)\,\mathrm{e}^{-BJ(J+1)hc/k_\mathrm{B}T}, \tag{1}$$

where J is the quantum number of the total angular momentum, N_J is the number of molecules in the rotational level J, T is the rotational temperature, B is the rotational constant of a rigid rotator, and k_B is the Boltzmann constant. Generally, by using a noble gas seeded a few molecules of interest for producing supersonic beam, rotational temperatures of the beam below 5 K can be obtained.[29] As can be seen from Fig. 2, the rotational states with $J=1$ contribute most to the total molecular population. Even at the rotational temperature of 10 K, 99.5% of the molecules reside at the $J=1$ ground rotational state in the beam.

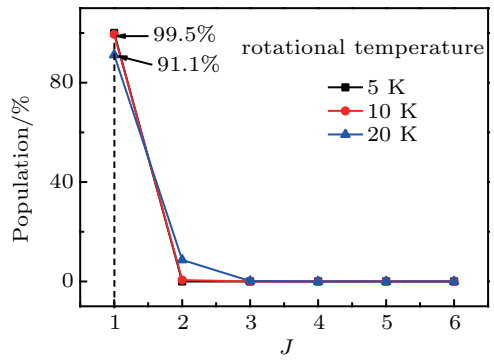


Fig. 2. The relative populations of the NH_3 molecules in different rotational states at the rotational temperatures of $T=5$ K, 10 K, and 20 K.

The NH_3 molecule in the states $|J,K,M\rangle = |1,1,\pm1\rangle$ has an electric dipole moment of 1.47 Debye directed along the molecular axis.[65] The Stark shifts of the molecule should also be known, with which we derive the forces needed to generate time sequences for the experiment and perform 3D MC trajectory simulations of the experiment. NH_3 is a kind of symmetric top molecule and has a pyramidal structure that allows a vibrational umbrella motion which leads to a splitting of $|J,K\rangle = |1,1\rangle$ level into a symmetric component and an anti-symmetric component by the tunneling effect along the umbrella motion. The energy difference between these two components, i.e., the inversion splitting E_inv, is 0.79 cm^{-1}.[55] In the presence of an external electric field, the symmetric and the anti-symmetric levels interact with each other, leading to four levels. In the deceleration experiments presented here, the Stark effect of NH_3 molecule can be approximated by just considering the interaction between the two inversion levels, thus the Stark energy of $|J,K\rangle = |1,1\rangle$ varying with the magnitude of the external electric field can be easily calculated using the equation[61]

$$E_\mathrm{Stark} = \frac{E_\mathrm{inv}}{2} \pm \sqrt{\left(\frac{E_\mathrm{inv}}{2}\right)^2 + \left(-\mu_\mathrm{eff}E\frac{MK}{J(J+1)}\right)^2}, \tag{2}$$

where E_Stark is the Stark energy, E_inv is the inversion splitting, μ_eff is the effective molecular dipole moment, J is the quantum number of the total angular momentum, M is the quantum number of the projection of the total angular momentum along the direction of the external electric field, K is the quantum number of the projection of the total angular momentum along the direction of the principle axis of inertia of the molecule, and E is the absolute electric field strength. The Stark energy levels of the rotational states $|J,K\rangle = |1,1\rangle$ of NH_3 and ND_3 are both shown in Fig. 3. Compared to the ND_3 molecule, it is more difficult to slow down the NH_3 molecule because of its relatively large inversion splitting. In this paper, the NH_3 molecules in the $|J,KM\rangle = |1,-1\rangle$ state are manipulated. At low electric fields, the inversion splitting gives rise to a quadratic dependence of the Stark shift of this state on the applied electric field. When the electric field becomes strong, the Stark interaction between the molecule and the applied field becomes large, compared to the zero-field splitting, and the Stark shift is linear.

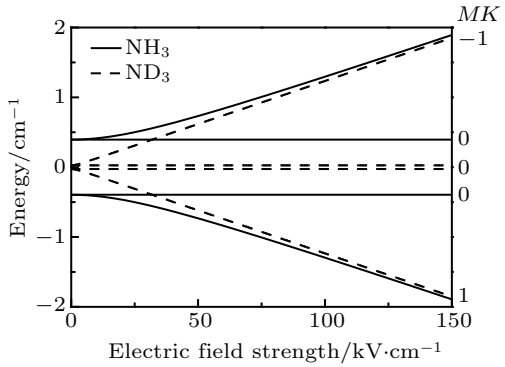


Fig. 3. The Stark shift of $|J,K\rangle = |1,1\rangle$ state of the NH_3 and ND_3 molecules in an electric field of up to 150 kV/cm.

3.2. Experimental results and analysis

In the experiments presented here, the decelerator is operated at voltages of +10 kV and −10 kV. The guiding mode is used to get the information about the center velocity and the velocity spread of the initial beam for deciding appropriate parameters refer to the dynamic simulations and the deceleration experiments, and the hexapole is applied with zero voltage in this mode.

Figure 4 shows time-of-flight (TOF) profiles of the NH_3 beam exiting the decelerator using the normal mode operation. The initial beam has a mean velocity of 338 m/s and a velocity spread FWHM of 65 m/s, corresponding to a translational

temperature of 1.6 K according to the relationship[66]

$$T = \frac{m(\Delta v_z)^2}{8\ln 2 \cdot k_B}, \tag{3}$$

where m is the mass of the molecule, Δv_z is the translational velocity spread of the molecular packet, and T is the corresponding translational temperature. However, the initial speed of the synchronous molecule determined by the switching sequence is always the same 333 m/s, which is a little different from the central velocity of 338 m/s. A hexapole 53.5 mm downstream the nozzle of the pulse valve is used to transversely focus the incident beams. Constant voltages of ±7.5 kV are applied to the electrodes of the hexapole when the decelerator is operated in the deceleration or bunching mode, resulting in an enhancement of the signals by a factor of 1.5. In Fig. 4, these observed TOF profiles are shown when the decelerator is operated at $\phi_0 = 0°, 10°, 20°, 30°, 40°, 45°$, and 48.36°, resulting in a packet of NH_3 molecules with a final velocity of 333 m/s, 301 m/s, 266 m/s, 218 m/s, 154 m/s, 98 m/s, and 18 m/s, respectively. Only the segment of the TOF profiles that contains the synchronous decelerated molecules is shown. For comparison, the TOF profile observed in guiding mode is also shown. As the synchronous phase angle is increased, the final speed of the slow packet decreases, and the packet arrives at a later time. The intensity of the peak also decreases mainly due to two reasons. First, the longitudinal phase-space acceptance decreases when the synchronous phase angle becomes larger, and thus the number of decelerated molecules decreases. Second, the slower the molecules, the more they spread out as they fly from the exit of the decelerator to the detection area. We finally obtain a decelerated packet of NH_3 molecules with a center velocity of 18 m/s, removing 99.7% of the kinetic energy, which is slow enough to be trapped in an electrostatic trap, and a spread FWHM of 8.9 m/s, corresponding to a translational temperature of 29.2 mK, as shown in the inset of Fig. 4.

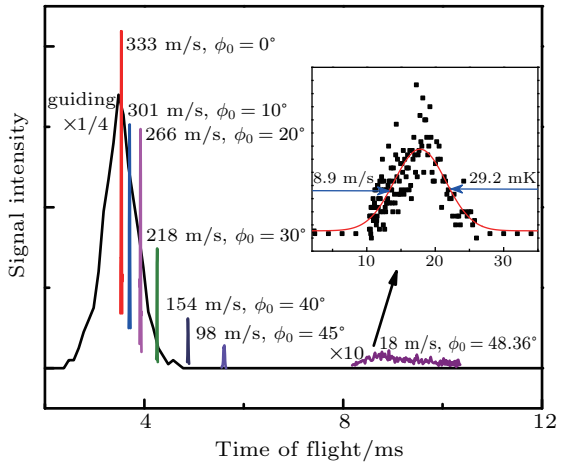


Fig. 4. Experimental TOF signals of NH_3 versus the synchronous phase angle. The inset shows the decelerated packet for $\phi_0 = 48.36°$, together with the velocity spread and the corresponding temperature of the packet.

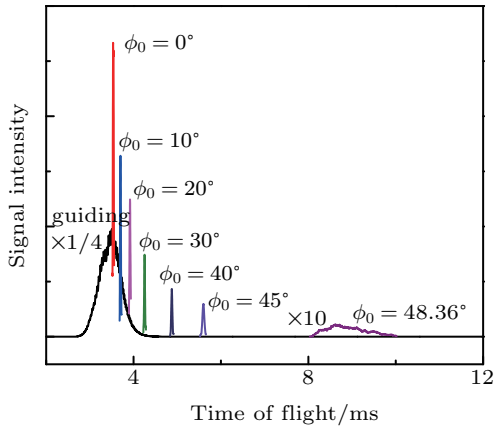


Fig. 5. Calculated TOF signals of NH_3 by three-dimensional Monte Carlo simulation when the decelerator is operated in the normal mode.

MC trajectory simulation can help us to understand the behavior of the Stark deceleration process.[29,35,40] The TOF profiles obtained by 3D MC trajectory simulations of the experiments are shown in Fig. 5, which are in good agreement with the experimental profiles shown in Fig. 4, except that the decelerated peaks in the calculated results are more intensity than those in the experimental data, compared to the respective guiding peaks, which results from the non-ideal conditions in the experiments concerning the actual voltages applied and the structural deviation of the decelerator. In these simulations, the initial molecular beams have Gaussian distributions in both spatial and velocity coordinates.

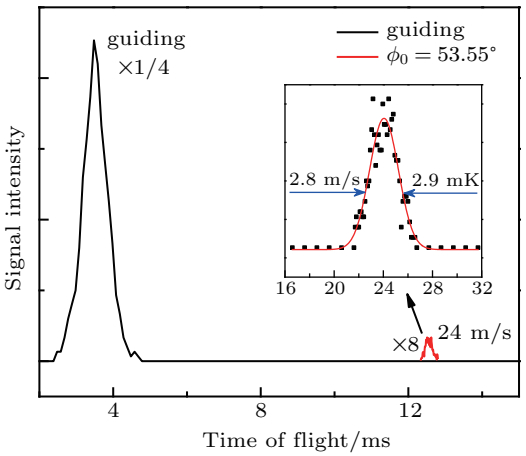


Fig. 6. Experimental TOF signals of NH_3 when the decelerator is operated in the deceleration-bunch mode. The inset is the zoom-in of the decelerated packet, together with the velocity spread and the corresponding temperature of the packet.

Figure 6 shows the TOF profiles of NH_3 in $|J, KM\rangle = |1, -1\rangle$ state exiting the decelerator under the deceleration-bunch mode operation. The experimental conditions are the same as the normal mode. We first decelerate the initial beam using 157 stages of the decelerator in the normal mode with a phase angle $\phi_0 = 53.55°$ to 24 m/s, and then bunch the slow beam using the remaining 22 stages in the bunching mode, leading to the velocity spread as narrow as 2.8 m/s, corresponding to a longitudinal temperature of just 2.9 mK which

is ten times lower than that of the packet obtained in the normal mode. 3D MC trajectory calculations for the experiments in this mode are also performed and agree with the observed data, as shown in Fig. 7.

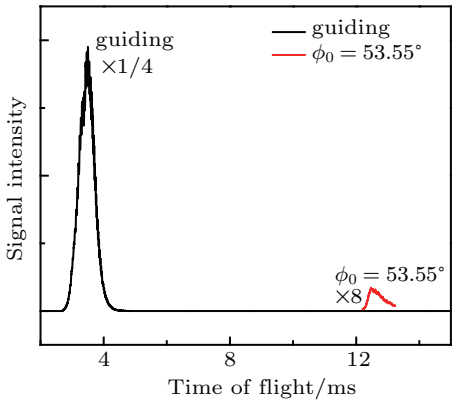


Fig. 7. Calculated TOF signals of NH_3 by 3D Monte Carlo simulation when the decelerator is operated in the deceleration-bunch mode.

4. Conclusion

We experimentally slowed supersonic beams of NH_3 molecules using our 179-stage Stark decelerator in two different operation modes, the normal mode and the deceleration-bunch mode. Starting from an initial speed of 333 m/s, the pulse beam of NH_3 molecules seeded in xenon was slowed down to 18 m/s in the normal mode with a synchronous phase angle $\phi_0 = 48.36°$, resulting in a slow packet with a velocity spread of 8.9 m/s, corresponding to a longitudinal temperature of 29.2 mK. Besides, the supersonic beam of NH_3 was also decelerated to 24 m/s in the deceleration-bunch mode with a phase angle $\phi_0 = 53.55°$ in slowing stages, leading to a colder decelerated packet with a narrower velocity spread of 2.8 m/s, corresponding to a temperature of 2.9 mK, lower than that of the packet obtained in the normal mode by 10 times. 3D MC trajectory simulations have also been performed and the simulated TOF profiles are in good agreement with the observed ones.

These Stark decelerated cold molecules of NH_3 can subsequently be trapped in electrostatic traps for some promising applications such as cold collision experiments,[58] high-resolution spectroscopy,[55] and precision measurements.[56,57] Several potential improvements can be made in the experiments. The voltage difference between the electrodes of the decelerator can be increased using the method of high-voltage conditioning with glow discharge of nitrogen and helium, and then the decelerator can be operated at higher voltages in the experiments, leading to more kinetic energy loss per stage. Besides, if the pulse valve is replaced by another one that can be operated down to liquid nitrogen temperatures, the valve can be cooled to a temperature much lower than room temperature such as 200 K, resulting in smaller initial central velocity of the molecular beam, which will also lead to the increase in the number of slow molecules.

References

[1] Carr L D, DeMille D, Krems R V and Ye J 2009 *New J. Phys.* **11** 055049
[2] Bell M T and Softley T P 2009 *Mol. Phys.* **107** 99
[3] Gilijamse J J, Hoekstra S, van de Meerakker S Y T, Groenenboom G C and Meijer G 2006 *Science* **313** 1617
[4] Sawyer B C, Stuhl B K, Yeo M, Tscherbul T V, Hummon M T, Xia Y, Klos J, Patterson D, Doyle J M and Ye J 2011 *Phys. Chem. Chem. Phys.* **13** 19059
[5] Kirste M, Wang X G, Schewe H C, Meijer G, Liu K, van der Avoird A, Janssen L M C, Gubbels K B, Groenenboom G C and van de Meerakker S Y T 2012 *Science* **338** 1060
[6] Willitsch S, Bell M T, Gingell A D, Procter S R and Softley T P 2008 *Phys. Rev. Lett.* **100** 043203
[7] Bell M T, Gingell A D, Oldham J M, Softley T P and Willitsch S 2009 *Faraday Discuss.* **142** 73
[8] Ospelkaus S, Ni K K, Wang D, de Miranda M H G, Neyenhuis B, Quéméner G, Julienne P S, Bohn J L, Jin D S and Ye J 2010 *Science* **327** 853
[9] Berteloite C, Lara M, Bergeat A, Le Picard S D, Dayou F, Hickson K M, Canosa A, Naulin C, Launay J M, Sims I R and Costes M 2010 *Phys. Rev. Lett.* **105** 203201
[10] van Veldhoven J, Küpper J, Bethlem H L, Sartakov B, van Roij A J A and Meijer G 2004 *Eur. J. Phys. D* **31** 337
[11] Hudson E R, Lewandowski H J, Sawyer B C and Ye J 2006 *Phys. Rev. Lett.* **96** 143004
[12] Hudson J J, Sauer B E, Tarbutt M R and Hinds E A 2002 *Phys. Rev. Lett.* **89** 023003
[13] Collaboration A C M E 2014 *Science* **343** 269
[14] Cairncross W B, Gresh D N, Grau M, Cossel K C, Roussy T S, Ni Y, Zhou Y, Ye J and Cornell E A 2017 *Phys. Rev. Lett.* **119** 153001
[15] Weinstein J D, deCarvalho R, Guillet T, Friedrich B and Doyle J M 1998 *Nature* **395** 148
[16] Bethlem H L, Berden G and Meijer G 1999 *Phys. Rev. Lett.* **83** 1558
[17] Vanhaecke N, Meier U, Andrist M, Meier B H and Merkt F 2007 *Phys. Rev. A* **75** 031402(R)
[18] Narevicius E, Libson A, Parthey C G, Chavez I, Narevicius J, Even U and Raizen M G 2008 *Phys. Rev. A* **77** 051401(R)
[19] Fulton R, Bishop A I and Barker P F 2004 *Phys. Rev. Lett.* **93** 243004
[20] Yamakita Y, Procter S R, Goodgame A L, Softley T P and Merkt F 2004 *J. Chem. Phys.* **121** 1419
[21] Hogan S D, Seiler Ch and Merkt F 2009 *Phys. Rev. Lett.* **103** 123001
[22] Shuman E S, Barry J F and DeMille D 2010 *Nature* **467** 820
[23] Hummon M T, Yeo M, Stuhl B K, Collopy A L, Xia Y and Ye J 2013 *Phys. Rev. Lett.* **110** 143001
[24] Zhelyazkova V, Cournol A, Wall T E, Matsushima A, Hudson J J, Hinds E A, Tarbutt M R and Sauer B E 2014 *Phys. Rev. A* **89** 053416
[25] Lim J, Almond J R, Trigatzis M A, Devlin J A, Fitch N J, Sauer B E, Tarbutt M R and Hinds E A 2018 *Phys. Rev. Lett.* **120** 123201
[26] Xu L, Yin Y, Wei B, Xia Y and Yin J 2016 *Phys. Rev. A* **93** 013408
[27] Prehn A, Ibrügger M, Glöckner R, Rempe G and Zeppenfeld M 2016 *Phys. Rev. Lett.* **116** 063005
[28] Bethlem H L, Berden G, Crompvoets F M H, Jongma R T, van Roij A J A and Meijer G 2000 *Nature* **406** 491
[29] Bethlem H L, Crompvoets F M H, Jongma R T, van de Meerakker S Y T and Meijer G 2002 *Phys. Rev. A* **65** 053416
[30] Bochinski J R, Hudson E R, Lewandowski H J, Meijer G and Ye J 2003 *Phys. Rev. Lett.* **91** 243001
[31] van de Meerakker S Y T, Labazan I, Hoekstra S, Küpper J and Meijer G 2006 *J. Phys. B: At. Mol. Opt. Phys.* **39** S1077
[32] Hudson E R, Ticknor C, Sawyer B C, Taatjes C A, Lewandowski H J, Bochinski J R, Bohn J L and Ye J 2006 *Phys. Rev. A* **73** 063404
[33] Jung S, Tiemann G and Lisdat C 2006 *Phys. Rev. A* **74** 040701(R)
[34] Tokunaga S K, Dyne J M, Hinds E A and Tarbutt M R 2009 *New J. Phys.* **11** 055038

[35] Wall T E, Kanem J F, Dyne J M, Hudson J J, Sauer B E, Hinds E A and Tarbutt M R 2011 *Phys. Chem. Chem. Phys.* **13** 18991

[36] Tarbutt M R, Bethlem H L, Hudson J J, Ryabov V L, Ryzhov V A, Sauer B E, Meijer G and Hinds E A 2004 *Phys. Rev. Lett.* **92** 173002

[37] Wohlfart K, Grätz F, Filsinger F, Haak H, Meijer G and Küpper J 2008 *Phys. Rev. A* **77** 031404(R)

[38] Wang X, Kirste M, Meijer G and van de Meerakker S Y T 2013 *Z. Phys. Chem.* **227** 1595

[39] van den Berg J E, Mathavan S C, Meinema C, Nauta J, Nijbroek T H, Jungmann K, Bethlem H L and Hoekstra S 2014 *J. Mol. Spectrosc.* **300** 22

[40] van de Meerakker S Y T, Smeets P H M, Vanhaecke N, Jongma R T and Meijer G 2005 *Phys. Rev. Lett.* **94** 023004

[41] Quintero-Pérez M, Jansen P, Wall T E, van den Berg J E, Hoekstra S and Bethlem H L 2013 *Phys. Rev. Lett.* **110** 133003

[42] Cheng C, van der Poel A P P, Jansen P, Quintero-Pérez M, Wall T E, Ubachs W and Bethlem H L 2016 *Phys. Rev. Lett.* **117** 253201

[43] Bethlem H L, van Roij A J A, Jongma R T and Meijer G 2002 *Phys. Rev. Lett.* **88** 133003

[44] Meek S A, Conrad H and Meijer G 2009 *Science* **324** 1699

[45] Osterwalder A, Meek S A, Hammer G, Haak H and Meijer G 2010 *Phys. Rev. A* **81** 051401(R)

[46] Meek S A, Parsons M F, Heyne G, Platschkowski V, Haak H, Meijer G and Osterwalder A 2011 *Rev. Sci. Instrum.* **82** 093108

[47] Hou S, Wang Q, Deng L and Yin J 2016 *J. Phys. B: At. Mol. Opt. Phys.* **49** 065301

[48] Shyur Y, Bossert J A and Lewandowski H J 2018 *J. Phys. B: At. Mol. Opt. Phys.* **51** 165101

[49] Wang Q, Hou S, Xu L and Yin J 2016 *Phys. Chem. Chem. Phys.* **18** 5432

[50] Foreman P 1985 *Proc. IEEE* **73** 1181

[51] Gordon J P, Zeiger H J and Townes C H 1954 *Phys. Rev.* **95** 282

[52] Gunther-Mohr G R, White R L, Schawlow A L, Good W E and Coles D K 1954 *Phys. Rev.* **94** 1184

[53] Gordon J P, Zeiger H J and Townes C H 1955 *Phys. Rev.* **99** 1264

[54] Shimoda K, Wang T C and Townes C H 1956 *Phys. Rev.* **102** 1308

[55] Kukolich S G 1967 *Phys. Rev.* **156** 83

[56] Bethlem H L, Kajita M, Sartakov B, Meijer G and Ubachs W 2008 *Eur. Phys. J. Spec. Top.* **163** 55

[57] Jansen P, Bethlem H L and Ubachs W 2014 *J. Chem. Phys.* **140** 010901

[58] Gubbels K B, van de Meerakker S Y T, Groenenboom G C, Meijer G and van der Avoird A 2012 *J. Chem. Phys.* **136** 074301

[59] Bickes Jr R W, Duquette G, van den Meijdenberg C J N, Rulis A M, Scoles G and Smith K M 1975 *J. Phys. B: At. Mol. Phys.* **8** 3034

[60] Jansen P, Quintero-Pérez M, Wall T E, van den Berg J E, Hoekstra S and Bethlem H L 2013 *Phys. Rev. A* **88** 043424

[61] van de Meerakker S Y T, Bethlem H L, Vanhaecke N and Meijer G 2012 *Chem. Rev.* **112** 4828

[62] Hudson E R, Bochinski J R, Lewandowski H J, Sawyer B C and Ye J 2004 *Eur. Phys. J. D* **31** 351

[63] Parazzoli L P, Fitch N, Lobser D S and Lewandowski H J 2009 *New J. Phys.* **11** 055031

[64] Herzberg G and Spinks J W T 1950 *Molecular Spectra and Molecular Structure I. Spectra of Diatomic Molecules* (New York: D. Van Nostrand Company Inc.) p. 124

[65] Gandhi S R and Bernstein R B 1987 *J. Chem. Phys.* **87** 6457

[66] Heiner C E 2009 *A Molecular Synchrotron* (Ph. D. Dissertation) (Berlin: Fritz-Haber-Institut der Max-Planck-Gesellschaft)